IEEE Photonics Journal
An IEEE Photonics Society Publication

Open Access

Real-Time Q-Band OFDM-RoF Systems With Optical Heterodyning and Envelope Detection for Downlink Transmission

Volume 9, Number 2, April 2017

Ming Chen
Jianjun Yu
Xin Xiao

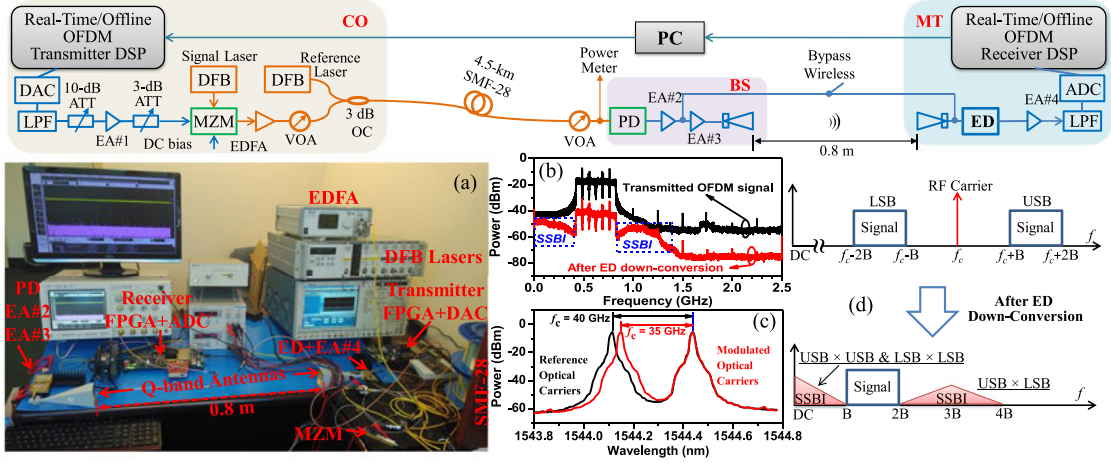

DOI: 10.1109/JPHOT.2017.2671870
1943-0655 © 2017 IEEE

IEEE photonics SOCIETY

IEEE

Real-Time Q-Band OFDM-RoF Systems With Optical Heterodyning and Envelope Detection for Downlink Transmission

Ming Chen,[1,2] Jianjun Yu,[1,3] and Xin Xiao[1]

[1]ZTE (TX) Inc., Morristown, NJ 07960, USA
[2]College of Physics and Information Science, Hunan Normal University, Changsha 410081, China
[3]Laboratory for Information Science of Electromagnetic Waves (MoE), Fudan University, Shanghai 200433, China

DOI:10.1109/JPHOT.2017.2671870

Manuscript received February 1, 2017; revised February 12, 2017; accepted February 14, 2017. Date of publication March 2, 2017; date of current version March 7, 2017. This work was supported in part by the National High-Tech Research and Development Program (863 Program) of China under Grant 2015AA016904 and in part by the National Natural Science Foundation of China under Grant 61325002 and Grant 61250018. Corresponding author: M. Chen (e-mail: ming.chen@hunnu.edu.cn).

Abstract: We experimentally demonstrate a real-time optical heterodyning and envelope detection-enabled orthogonal frequency-division-multiplexing-based Q-band radio-over-fiber (OFDM-RoF) system. Envelope-detector-based down-conversion is applied to the mobile terminal (MT), which makes MT insensitive to the phase noise of the beating millimeter wave signal and enables the generation of RoF signals using two free-running non-narrow line-width distributed feedback lasers in the central office. The error-free transmission real-time Reed–Solomon- coded 16-quadrature-amplitude modulation(16-QAM)-OFDM-RoF signals with a net bit rate of 1.2 Gb/s at 35/40 GHz over 4.5-km single-mode fiber (SMF) and 0.8-m wireless distance is reported in this paper. Additionally, the transmission performance of the signals at 35 GHz with the net bit rate from 1.5 to 5.9 Gb/s is also investigated by offline digital signal processing approaches. It indicates that the BER of the signal with the net rate up to 4.4 Gb/s after the SMF and wireless link transmission is below a 7% hard-decision forward error correction (FEC) threshold of 3.8×10^{-3}.

Index Terms: Radio over fiber (RoF), orthogonal frequency-division multiplexing (OFDM), Q-band, optical heterodyning, envelope detection.

1. Introduction

In recent years, radio over fiber (RoF) has been regarded as a cost-effective technique for future broadband wireless access networks. It has attracted much attention from both industry and academia, mainly due to its numerous attractive features such as high bandwidth, extended coverage, and simplified base station (BS) [1], [2]. Meanwhile, orthogonal frequency-division multiplexing (OFDM) with high quadrature amplitude modulation (QAM) formats has been applied to RoF systems to combat fiber dispersion as well as improve spectral efficiency and capacity [3].

The generation of optical millimeter-wave (MW) signals in the central office (CO) and down-conversion of the generated MW-signal in mobile terminals (MTs), which are two key technologies for its applications and have been extensively studied [4]–[10]. Generally, the broadband external modulator, such as the Mach-Zehnder modulator (MZM), combined with narrow line-width

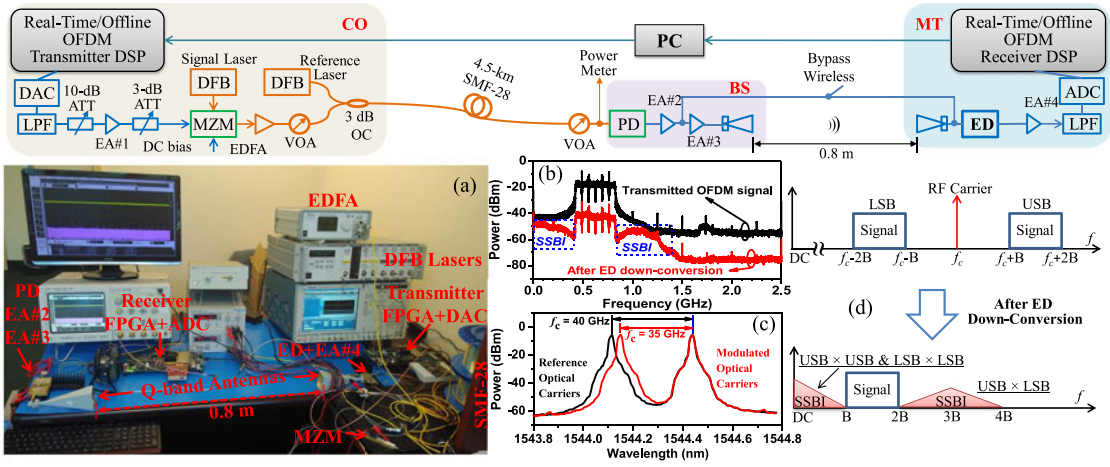

Fig. 1. Experimental setup of real-time/offline Q-band OFDM-RoF system with optical heterodyning and envelope detection for downlink transmission.

lasers (e.g., external-cavity laser, ECL), are employed to generate optical MW signals, and mixer down-conversion is applied in MTs [4]. However, as the carrier frequency increases, the power of local oscillator (LO) located in MTs may be limited for down-conversion using mixer due to the amplifier [5], which makes MTs more complex, expensive and power-hungry. Instead of mixer down-conversion, envelope detector (ED) down-conversion enabled MT with better sensitivity than self-heterodyning [11], has been proposed for W-band RoF systems [5], [12]. It doesn't need LO in MT and is insensitive to phase noise of the generated MW-signals. Therefore, the non-narrow line-width lasers, such as distributed feedback lasers (DFBs) and directly-modulated lasers (DMLs), can be used to generate the optical MW signals to further enhance the cost-effectiveness of the RoF systems. In [10] and [11], the optical MW signals have been generated by heterodyning two free-running laser signals with a wavelength difference of the desired carrier frequency, using external modulation and direct modulation, respectively. It is very flexible to achieve the desired MW carrier frequency after photo-detection in BS over the whole microwave band by tuning the output wavelength of the signal laser or/and the reference laser. However, as far as we know, the real-time demonstration of the OFDM-RoF with optical heterodyning and envelope detection is seldom reported in this field. It is interesting to investigate this technique by using real-time DSP approaches before it can be deployed in application scenarios.

Recently, we have experimentally demonstrated real-time X-band (8-12 GHz) OFDM-RoF systems with both homodyne detection [13] and heterodyne detection [14] employing mixer down-conversion for uplink transmission. In this paper, we report a simple real-time Q-band (33-50 GHz) OFDM-RoF system with optical heterodyning and envelope detection techniques for downlink transmission. First, the optimal bias voltage for MZM modulator and optimal reference laser output power is determined by minimizing the bit error rate (BER) of the net bit rate of 1.2 Gb/s 16-QAM-OFDM-RoF signals at 40 GHz after 4.5 km SMF-28 transmission. Then, the BER stability of the RoF systems is investigated. Finally, after 4.5 km SMF-28 and 0.8-m wireless transmission, the BER and error vector magnitude (EVM) performances of 1.2 Gb/s real-time RoF signals and up to 5.9 Gb/s offline RoF signals are discussed.

2. Experimental Setup

The performance of the proposed Q-band OFDM-RoF system with optical heterodyning and envelope detection for downlink transmission is experimentally investigated by both real-time and offline methods. The experimental setup is illustrated in Fig. 1. Fig. 1(a) is the photograph of the real-time OFDM-RoF system. For the real-time experiments, the detailed OFDM transceiver DSP

algorithms can be found in our previous work [14], including Reed-Solomon (RS) encoding with RS (255, 223), symbol interleaving, 16-QAM mapping, pilot insertion, 256-point IFFT, digital clipping, adding cyclic prefix (CP), synchronization pattern and training sequences (TSs), and digital I/Q modulation at the transmitter, and 2:1 resampling, I/Q demodulation, 4:1 resampling, timing synchronization, CP removal, 64-point FFT, TS-based single-tap channel estimation and equalization, 16-QAM de-mapping, symbol de-interleaving and RS decoding. The key digital OFDM parameters are summarized as follows: Only 40 of 256 subcarriers (SCs) consists of 36 data-carrying SCs and 4 pilot SCs is used with indices from -20 to -1 and 1 to 20. Here, pilot SCs are reserved for sampling frequency offset (SFO) compensation [15] in case the SFO is large enough. However, the SFO compensation isn't engaged in this experiment due to the very small SFO existing. Other high-frequency 215 SCs are filled with zeros for oversampling. DC SC is also filled with zero, and CP length is 16. The OFDM frame consists of one 256-sample synchronization pattern, four TSs, and 255 data-carrying OFDM symbols.

In the CO, the complex-valued outputs from IFFT module are I/Q modulated to a digital intermediate-frequency (IF) signal, and then converted to an analog one by a 14-bit DAC operating at a sampling rate of 2.5 GS/s. The converted signal centered at 625 MHz IF, with $\sim$400 MHz bandwidth and $\sim$700 mV peak-to-peak voltage, is filtered by a 1 GHz, low-pass filter (LPF) to remove the alias components created by DAC conversion, and then attenuated by a 10 dB electrical fixed attenuator (ATT). The attenuated signal is amplified by a 10 GHz RF amplifier (EA#1, JDSU H301), attenuated by the second 3 dB ATT, and then used as a drive to a 40 Gb/s single-electrode MZM. The electrical spectrum of the attenuated OFDM signal (solid black line) is plotted in Fig. 1(a), where a guard band about 400 MHz around direct current (DC) component, is generated to avoid subcarrier-to-subcarrier beating interference (SSBI). The optical source for the MZM, as the signal laser, is a tunable distributed feedback laser (DFB) with line-width of 5 MHz, output power of 12 dBm and center wavelength of 1544.44 nm. The output optical double-sideband (ODSB) signal from the MZM is boosted by an erbium-doped fiber amplifier (EDFA) with 5 dB noise figure, and then attenuated by a variable optical attenuator (VOA) to 7 dBm. The ODSB signal is combined with another tunable DFB with a line-width of 5 MHz, output power of 7 dBm and center wavelength of 1544.12 nm (1544.16 nm) via 3 dB optical coupler (OC), and launched into 4.5 km SMF-28. The wavelength difference between the signal laser and reference laser is chosen to obtain the desired 40 GHz (35 GHz) MW carrier frequency, f_c. The corresponding optical spectra are presented in Fig. 1(b). The net bit rate (R) of the real-time systems can be expressed as

$$R = (N_{DSC} * \log2(M) * N_{DS} * R_S) / (L_{SP} + N_{TS} * L_{TS} + N_{DS} * (N + L_{CP})) / (1 + OH_{FEC})$$

where N_{DSC} denotes the number of data-carrying SCs, M is the order of QAM modulation, R_S is the DAC sampling rate, L_{SP}, L_{TS} and L_{CP} are the lengths of synchronization pattern, training sequence and CP, respectively. N_{TS} and N_{DS} are the numbers of the TS and data-carrying OFDM symbols in an OFDM frame, and N is the size of IFFT. Here, $N_{DSC} = 36$, $M = 16$, $N_{DS} = 255$, $R_S = 2.5\,GS/s$, $L_{SP} = 256$, $N_{TS} = 4$, $L_{TS} = 272$, $N = 256$, and $L_{CP} = 16$. Since RS (255, 223) is used, OH_{FEC} is 14%. Thus, R is 1.14 Gb/s.

After SMF transmission, the received ODSB signal is attenuated by the second VOA, then converted to MW-signal by a 50 GHz photo-detector (PD). The MW-signal is amplified by an electrical amplifier (EA#2, SHF 818, 32 dB gain @ 36–41 GHz). In the case of no wireless transmission (i.e. cable transmission), the amplified signal is directly fed into a Q-band envelope detector (ED, Millitech DXP-22-0). In the wireless delivery case, the amplified signal is amplified again by a broadband amplifier (EA#3, SHF 804 EA, 20 dB gain @30 kHz–45 GHz) before being sent to a Q-band antenna with 3 dB beam-width of 10° for 0.8 m wireless transmission. In the MT, the MW signal is received by another antenna in the case of wireless transmission, down-converted with ED, amplified by the 4th EA (EA#4, SHF 826H) with 25 GHz BW and 25 dB gain, and filtered by a 1 GHz LPF. Subsequently, the filtered signal is sampled by a 10-bit ADC working at 5 GS/s, and sent to receiver FPGA for real-time OFDM demodulation. The principle of the SSBI effect after ED down-conversion is sketched in Fig. 1(c). We can see clearly from the spectrum of ED down-converted OFDM signal

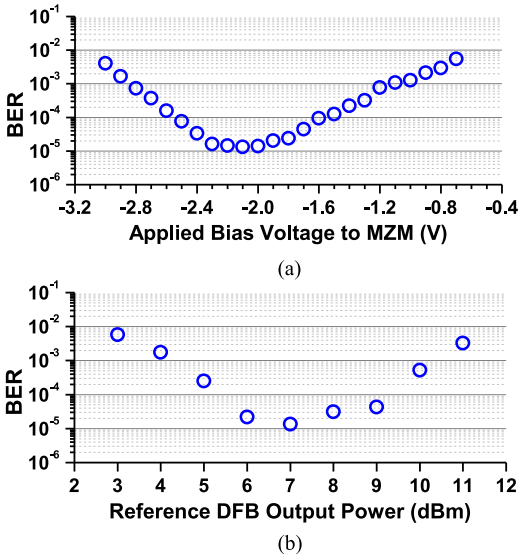

Fig. 2. Real-time measured BER curves versus (a) applied bias voltage to MZM and (b) reference DFB laser output power.

(solid red line), as shown in Fig. 1(a), that the unwanted SSBIs fall at frequencies both below and above the wanted data-carrying OFDM SCs.

For the offline experiments, the DSP algorithms for OFDM modulation and demodulation are the same as the real-time experiments, except for RS encoding/decoding. RS coding isn't engaged in the offline transceiver. A commercial arbitrary waveform generator (AWG, Tektronix AWG7122B) with 10-bit resolution operates at sampling rates from 3 to 12 GS/s, which is used as DAC. Analog-to-digital conversion is implemented by an 8-bit, 13 GHz digital storage oscilloscope (DSO, Agilent DSO81304B) operating at the sampling rate of 20 GS/s. It should be noticed that the ratio of the first resampling operation as mentioned above is depended on the AWG sampling rate. For example, if the AWG sampling rate is 5 GS/s, the 4:1 resampling should be implemented in the first resampling operation.

3. Experimental Results and Discussion

The transmission performances of the proposed Q-band OFDM-RoF system are investigated in the following three cases: (1) only 4.5 km SMF-28 transmission, (2) 4.5 km SMF-28 and 0.8 m wireless transmission, and (3) offline experiments with higher data rate.

3.1 Only 4.5 km SMF-28 Transmission

After only 4.5 km SMF-28 transmission, the received optical power (ROP) is fixed at -1 dBm, the reference laser output power is set to 7 dBm and MW carrier frequency is 40 GHz, the real-time measured BER as a function of the applied bias voltage of MZM is shown in Fig. 2(a). The optimum bias voltage is about 2.1 V when the BER is minimized to around 1×10^{-5}. Thus, the optimum bias voltage is applied to MZM for the following measurements. Fig. 2(b) shows the real-time measured BER as a function of the output power of reference DFB laser. It indicates that the optimum reference laser output power is 7 dBm, which is the same as the ODSB signal. The real-time BERs are calculated by counting over 65536 OFDM frames containing more than 2×10^9 information-bearing bits.

Fig. 3 shows the BER performances of the proposed RoF system operating at both 35 and 40 GHz versus ROP under optimum reference laser output power for optical back-to-back (OB2B)

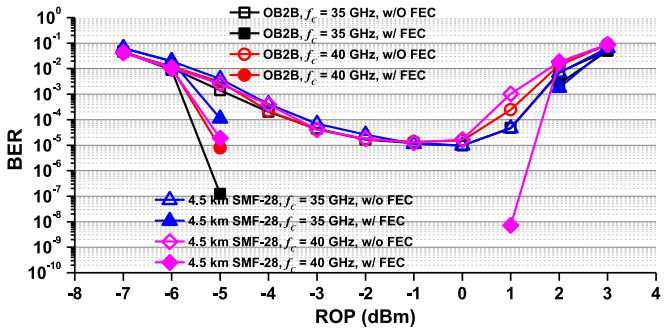

Fig. 3. Real-time measured BER versus ROP for no wireless transmission.

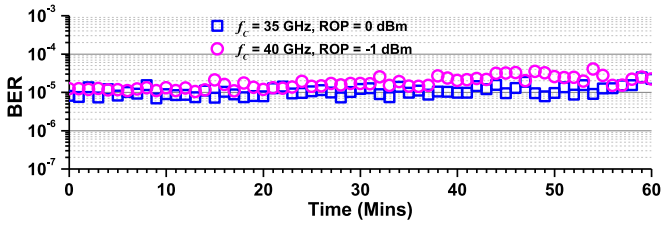

Fig. 4. BER performance stability.

and 4.5 km SMF-28 transmission cases. The power penalties are negligible after SMF transmission for both 35 and 40 GHz uncoded OFDM-RoF systems. The optimum ROPs are 0 and 1 dBm for 35 and 40 GHz RoF systems, respectively. When the ROPs are greater than the optimum ROPs, the degraded BER performance is mainly attributed to the nonlinear distortion induced by gain-saturation of EA#2. Because the dynamic range of the ADC is limited to $-250 \sim 250$ mV, the ADC clipping effects will occur if the maximal input signal exceeds the ADC's dynamic range, which may be another reason for the BER degradation. It should be mentioned that the BERs are all zeros for RS-coded systems as the ROPs between -4 to 0 dBm. It also exhibits that the BER threshold of the forward error correction (FEC) scheme, i.e., RS (255, 223), is around 1×10^{-3} for the no wireless transmission cases.

To investigate the stability of the proposed system, the BERs for the 35 and 40 GHz systems at optimum ROPs of 0 and -1 dBm, are real-time measured every minute for one hour. The BER performance of uncoded systems as a function of time in minutes is presented in Fig. 4, while the error-free transmissions are observed for RS-coded systems. As we can see, the BER performances are slightly degraded in the experimental measurement period. This fact is due to the MZM bias drift. In practical applications, a bias controller should be implemented to compensate this effect.

3.2 4.5 km SMF-28 and 0.8 m Wireless Transmission

After additional 0.8 m wireless transmission, the real-time measured BER performances of both the RS uncoded and coded proposed systems, as functions of ROP, are shown in Fig. 5. The power penalty is negligible compared to the no wireless transmission case. The 16-QAM constellation diagrams for the 20th SC of both 35 and 40 GHz OFDM-RoF systems at ROP of 0 and -1 dBm are shown in Figs. 5(a) and (b), respectively.

3.3 Offline Experiments With Higher Data Rate

The net bit rate of the proposed real-time Q-band OFDM-RoF system is about 1 Gb/s, which is mainly due to the limited bandwidths of the employed DAC and ADC. To evaluate the transmission

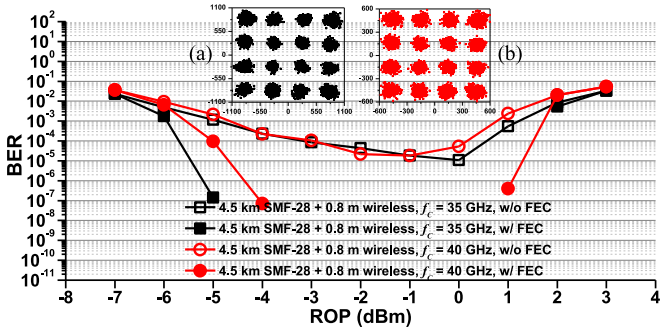

Fig. 5. Real-time measured BER versus ROP for wireless transmission.

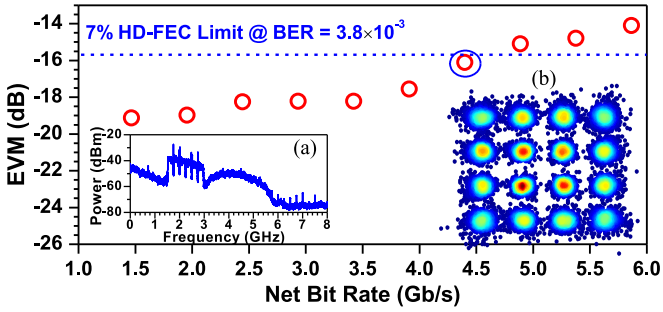

Fig. 6. Offline measured EVM performance versus net bit rate.

performance of the higher data rate of OFDM-RoF signal at 35 GHz, the offline experiments are also implemented, and the EVM performance as a function of the net bit rate is shown in Fig. 6. Here, the hard-decision forward error correction (HD-FEC) limit with the BER threshold of 3.8×10^{-3} is considered, and 400 data-carrying OFDM symbols are transmitted over OFDM frame duration, so the OH_{FEC} and N_{DS} are 7% and 400, respectively. The net bit rate for the offline experiments can be calculated by above-mentioned expression with $R_S = 3, 4, \ldots, 12\,GS/s$. It shows that the transmission of OFDM-RoF signal at 35 GHz with a maximum bit rate of 4.4 Gb/s over 4.5 km SMF-28 and 0.8 m wireless can be achieved with the BER under the 7% HD-FEC limit of 3.8×10^{-3}, the corresponding EVM is 15.6 dB [16]. Also, the spectrum and constellation diagram of the 4.4 Gb/s received signal are shown in Fig. 6(a) and (b), respectively. In the offline experiments, the net bit rate is limited by the AWG's bandwidth. There are some alternative ways to generate the OFDM-RoF signal with higher data rate up to tens of gigabits per second, such as analog I/Q up-conversion as described in [5]. We will focus on investigating the transmission performance of real-time OFDM-RoF at higher data rates in our future works.

4. Conclusion

In this paper, real-time 1.14 Gb/s Q-band OFDM-RoF systems using optical heterodyning and envelope detection for downlink transmission, is experimentally demonstrated for the first time. The optical MW signal is generated by heterodyning two free-running commercial DFB laser signals with a combined line-width of 10 MHz in CO and the down-conversion of the MW signal is implemented by a Q-band envelope detector in MT. The real-time measured BER performance showed that the proposed RS-coded OFDM-RoF signals error-free transmission over 4.5 km SMF-28 and 0.8 m wireless link can be successfully achieved with negligible power penalty, compared to OB2B configuration. Offline experiments with higher net bit rates up to 5.9 Gb/s, are also performed, and the results indicated that the BER of the OFDM-RoF signal at 35 GHz with a net bit rate

up to 4.4 Gb/s after the same SMF and wireless link transmission is below the HD-FEC limit of 3.8×10^{-3}.

References

[1] L. Chen *et al.*, "A radio-over-fiber system with a novel scheme for millimeter-wave generation and wavelength reuse for up-link connection," *IEEE Photon. Technol. Lett.*, vol. 18, no. 19, pp. 2056–2058, Oct. 2006.

[2] J. Yu *et al.*, "A novel radio-over-fiber configuration using optical phase modulator to generate an optical mm-wave and centralized lightwave for uplink connection," *IEEE Photon. Technol. Lett.*, vol. 19, no. 3, pp. 140–142, Feb. 2007.

[3] A. Stohr *et al.*, "High spectral-efficient 512-QAM-OFDM 60 GHz CRoF system using a coherent photonic mixer (CPX) and an RF envelope detector," presented at the Opt. Fiber Commun. Conf., Anaheim, CA, USA, 2016, Paper Tu3B.4.

[4] X. Li *et al.*, "W-band 8QAM vector signal generation by MZM-based photonic frequency octupling," *IEEE Photon. Technol. Lett.*, vol. 27, no. 12, pp. 1257–1260, Jun. 2015.

[5] C. Li *et al.*, "W-band OFDM RoF system with simple envelope detector down-conversion," presented at the 2015 Opt. Fiber Commun. Conf., Los Angeles, CA, USA, Paper W4G.6.

[6] J. Li *et al.*, "Millimeter-wave radio-over-fiber system based on two-step heterodyne technique," *Opt. Lett.*, vol. 34, no. 20, pp. 3136–3138, 2009.

[7] A. Kanno *et al.*, "40 Gb/s W-band (75–110 GHz) 16-QAM radio-over-fiber signal generation and its wireless transmission," *Opt. Exp.*, vol. 19, no. 26, pp. B56–B63, 2011.

[8] H. C. Chien *et al.*, "Optical millimeter-wave generation and transmission without carrier suppression for single- and multi-band wireless over fiber applications," *J. Lightw. Technol.*, vol. 28, no. 16, pp. 2230–2237, Aug. 2010.

[9] Y. Shao *et al.*, "Generation of 16-QAM-OFDM signals using selected mapping method and its application in optical millimeter-wave access system," *IEEE Photon. Technol. Lett.*, vol. 24, no. 15, pp. 1301–1303, Aug. 2012.

[10] A. H. M. R. Islam *et al.*, "Millimeter-wave radio-over-fiber system based on heterodyned unlocked light sources and self-homodyned RF receiver," *IEEE Photon. Technol. Lett.*, vol. 23, no. 8, pp. 459–461, Apr. 2011.

[11] I. Aldaya *et al.*, "Phase-insensitive RF envelope detection allows optical heterodyning of MHz-linewidth signals," *IEEE Photon. Technol. Lett.*, vol. 25, no. 22, pp. 2193–2196, Nov. 2013.

[12] X. Li *et al.*, "Performance improvement by pre-equalization in W-band (75-110GHz) RoF system," presented at the Opt. Fiber Commun. Conf., Anaheim, CA, USA, 2013, Paper OW1D.3.

[13] M. Chen *et al.*, "Demonstration of software-reconfigurable real-time FEC-enabled 4/16/64-QAM-OFDM signal transmission in an X-band RoF system," *IEEE Photon. J.*, vol. 8, no. 2, Apr. 2016, Art. ID. 7902908.

[14] M. Chen *et al.*, "Real-time generation and reception of OFDM signals for X-band RoF uplink with heterodyne detection," *IEEE Photon. Technol. Lett.*, vol. 29, no. 1, pp. 51–54, Jan. 2017.

[15] M. Chen *et al.*, "Symbol synchronization and sampling frequency synchronization techniques in real-time DDO-OFDM systems," *Opt. Commun.*, vol. 326, pp. 80–87, 2014.

[16] R. A. Shafik *et al.*, "On the extended relationships among EVM, BER and SNR as performance metrics," in *Proc. Int. Conf. Electr. Comput. Eng.*, 2006, pp. 408–411.